Journal of Applied Microbiology

Journal of Applied Microbiology ISSN 1364-5072

ORIGINAL ARTICLE

Excellent antimicrobial properties of silver-loaded mesoporous silica SBA-15

L. Wang[1], H. He[1], C. Zhang[1], L. Sun[1], S. Liu[1] and R. Yue[2]

1 Research Center for Eco-Environmental Sciences, Chinese Academy of Sciences, Beijing, China
2 Institute of Process Engineering, Chinese Academy of Sciences, Beijing, China

Keywords
antimicrobial activity, *E. coli*, reactive oxygen species, SBA-15, silver.

Correspondence
Hong He, Research Center for Eco-Environmental Sciences, Chinese Academy of Sciences, Beijing 100085, China.
E-mail: honghe@rcees.ac.cn

2013/1963: received 25 September 2013, revised 2 December 2013 and accepted 7 January 2014

doi:10.1111/jam.12443

Abstract

Aims: To synthesize silver-loaded mesoporous silica SBA-15 (Ag/SBA-15) materials and examine their antimicrobial action and antimicrobial mechanism.

Methods and Results: Ag/SBA-15 materials were prepared by means of incipient wetness impregnation, impregnation and direct hydrothermal synthesis methods. The antimicrobial activity of Ag/SBA-15 was investigated using *Escherichia coli* as an indicator bacterium, and the antimicrobial mechanism was explored. The properties and Ag^+ release behaviour of Ag/SBA-15 materials were compared. Experimental results showed that Ag/SBA-15 materials resulted in 7·5 log inactivation of *E. coli* for only 60 min, which exhibited very high antimicrobial activities at room temperature without using any light or electrical power input. The cell wall and cell membrane were destroyed in the antimicrobial process, leading to leakage of intracellular components. The formation of extracellular reactive oxygen species (ROS) involved in the bactericidal process was confirmed. Production of intracellular ROS was also discovered.

Conclusions: Ag/SBA-15 exhibited high antimicrobial activity against *E. coli*. This antimicrobial effect was a synergistic action between extracellular ROS and the toxicity of Ag^+, which induced intracellular ROS production and subsequent cell death.

Significance and Impact of the Study: This study revealed for the first time the antimicrobial activities and mechanisms of Ag/SBA-15 materials prepared with different methods.

Introduction

Human beings are often exposed to and infected by micro-organisms such as bacteria, moulds and viruses during day to day living. Accordingly, the use of antimicrobial agents is important to maintain a sanitary environment and avoid infection. Among various antimicrobial metals, silver has a wide antimicrobial spectrum and relatively high safety (TIC 1998). Concerns have been raised, however, regarding the bactericidal activity of silver nanoparticles that exhibit considerable antibacterial activity (Sondi and Salopek-Sondi 2004; Chamakura *et al.* 2011; Ivanova *et al.* 2011; Kim *et al.* 2011; Schacht *et al.* 2012). A comprehensive review on the antimicrobial action and mechanism of silver nanoparticles has been reported by Rai *et al.* (2012). However, silver nanoparticles usually gather into large particles, leading to a decrease in antimicrobial activity. To decrease silver usage and cost and increase the stability of antimicrobial agents, it is necessary to load silver onto inorganic carriers. Recently, many environmentally friendly inorganic antibacterial materials containing silver have been developed, with some now in commercial use (Kawahara *et al.* 2000; Wan *et al.* 2001; He *et al.* 2004; Pape *et al.* 2004; Chang *et al.* 2008a,b; Kwakye-Awuah *et al.* 2008; Lalueza *et al.* 2011). Therefore, the development of inorganic bactericides and disinfectants by loading silver onto various inorganic carriers is receiving

extensive attention for application in domestic and industrial fields.

Mesoporous silicas, such as SBA-15, possessing high surface area, porous volume and adjustable pore size diameter, are ideal supports. Their remarkably high surface area favours the high dispersion of active components on the support surface, and the improved accessibility of active sites for reaction gases should have a favourable impact on catalytic activity (Sayari 1996; Tian *et al.* 2009). Furthermore, if antimicrobial metals could be confined in the mesopores of SBA-15, the elution amount of metals might be largely reduced. Because of its excellent properties as a catalytic support, SBA-15 is one of the most promising carriers for the development of high-performance antimicrobial materials. Antimicrobial material using silver nanocrystals encapsulated in mesoporous silica MCM-41 has been prepared previously and was found to exhibit high antimicrobial efficacy against bacteria (Liong *et al.* 2009). Cai *et al.* (2006) prepared silver-loaded SBA-15 material through a silver mirror reaction and used it as an effective bactericide against *Staphylococcus*. Up to now, reports on the interaction of silver-loaded mesoporous silicas with bacteria are rare, and the antimicrobial mechanism remains unclear. Therefore, further work is needed to study the antimicrobial activity, antimicrobial mechanism and chemical durability of silver-loaded mesoporous silica.

Our previous work explored the efficiency of silver-loaded bactericidal materials including Ag/Al_2O_3, $AgCl/Al_2O_3$ and $Ag\text{-}Ce/AlPO_4$ in the inactivation of SARS coronavirus, *Escherichia coli* and yeast (He *et al.* 2004; Yan *et al.* 2005; Chang *et al.* 2007, 2008a,b; Chen *et al.* 2007). These micro-organisms could be completely inactivated within 30 min on the Ag/Al_2O_3 surface at room temperature in air. When Ag/Al_2O_3 was used in water, the elution of Ag^+ from the catalyst into water was a problem. Although $Ag\text{-}Ce/AlPO_4$ could significantly decrease the elution of Ag^+, the catalyst showed only moderate bactericidal activity. Therefore, to develop an excellent antibacterial material with high antimicrobial activity and chemical durability, silver-loaded mesoporous silica SBA-15 (Ag/SBA-15) antimicrobial materials were prepared by incipient wetness impregnation (Ag/SBA-15(IWI)), impregnation (Ag/SBA-15(I)) and direct hydrothermal synthesis (Ag/SBA-15(DHS)). It was expected that the incipient wetness impregnation method would decrease the elution of Ag^+ from the antimicrobial material into water by immobilizing Ag in the pores of SBA-15. Using *E. coli* as an indicator bacterium, the antimicrobial activities and mechanism of the Ag/SBA-15 materials were investigated by examining the diameter of the inhibition zone, bactericidal activity, effects of ROS and Ag^+ and morphological changes during the process of cell death.

Materials and methods

Preparation of Ag/SBA-15

The mesoporous silica SBA-15 was prepared as per previous research (Yang *et al.* 2007). To prepare pure SBA-15, 9 ml of tetraethoxy orthosilicate (TEOS, Sigma-Aldrich, St Louis, MO, USA) was added to 120 ml of 1 mol l^{-1} HNO_3 solution containing 4 g of triblock poly(ethylene oxide)-poly(propylene oxide)-poly(ethylene oxide) ($EO_{20}PO_{70}EO_{20}$, P123, Aldrich). The mixture was stirred for 24 h at 40°C and aged at 100°C overnight in Teflon bottles. The solid material obtained after filtering was finally calcined in air at 550°C for 3 h.

For the incipient wetness impregnation, preparation of Ag/SBA-15, SBA-15 was mixed with an appropriate volume of solution containing the required amount of silver nitrate. The sample was then dried in ambient air at 100°C overnight and calcined in air at 550°C for 3 h. The obtained sample was denoted as Ag/SBA-15(IWI).

For the impregnation, preparation of Ag/SBA-15, SBA-15 powder was introduced into an appropriate amount of silver nitrate aqueous solution, and the mixture was then stirred at room temperature followed by evaporation to dryness in a rotary evaporator at 60°C under reduced pressure. The resulting paste was dried at 100°C overnight and then calcined in air at 550°C for 3 h. The sample was denoted as Ag/SBA-15(I).

For the direct hydrothermal synthesis preparation of Ag/SBA-15, 4 g of P123 was dissolved in 120 ml of 1 mol l^{-1} HNO_3 solution for 3 h at 40°C. An appropriate amount of silver nitrate powder was introduced into the solution, which was stirred until it became clear. Then, 9 ml of TEOS was slowly added. The solution was stirred for 20 h at 40°C, and the mixture was aged for 24 h at 100°C. The resulting solid obtained after filtration was calcined at 550°C for 3 h. The sample was denoted as Ag/SBA-15(DHS).

Characterization of Ag/SBA-15

Scanning electron microscope (SEM) images and chemical composition analyses were obtained using a microscope (S-3000N; Hitachi, Tokyo, Japan) coupled with an energy dispersive X-ray (EDX) attachment. The content of Ag in Ag/SBA-15 was confirmed by EDX measurement. The accelerating voltage was 5·0 kV. Transmission electron microscope (TEM) photographs were taken with a Hitachi H-7500 electron microscope (Tokyo, Japan) at an operating voltage of 80 kV.

Surface area and pore size distribution of Ag/SBA-15 samples were determined through nitrogen adsorption/desorption isotherms at −196°C using a Quantasorb-18

automatic instrument (Quanta Chrome Instrument Co. Boynton Beach, FL, USA). All samples were initially outgassed for 6 h at 300°C in a vacuum. The specific surface areas were calculated from these isotherms by applying the Brunauer-Emmett-Teller (BET) method. Pore size distribution and mesopore volume (V_{meso}) were evaluated by applying the Dollimore–Heal method to the desorption isotherm (Dollimore and Heal 1964), and the *t*-plot approach (Lippens and Boer 1965) was adopted to estimate micropore volume (V_{micro}).

Culture of *Escherichia coli*

The *E. coli* K12 (ATCC 23716) bacterial strain was inoculated into lactose broth (LB) (Fluka Co. 61748, Buchs, Switzerland) and cultured aerobically for 24 h at 37°C with constant agitation. Aliquots of the culture were inoculated into fresh medium and incubated at 37°C for 12 h until they reached the exponential growth phase. Bacterial cells were collected after centrifugation, and the pellet was then washed and resuspended with sterilized water. Finally, bacterial cells were diluted with sterilized water and immediately plated on LB agar plates. The colonies were counted after incubation at 37°C for 24 h. A cell density corresponding to 10^9–10^{10} colony-forming units per millilitre (CFU ml^{-1}) was then achieved.

Test of antimicrobial activity

One millilitre of *E. coli* suspension was added to the conical flask containing 99 ml of sterilized water, and the as-prepared Ag/SBA-15 were then added to the system. The final Ag/SBA-15 concentration was adjusted to 50 mg l^{-1}, and the final cell concentration was 10^7–10^8 CFU ml^{-1}. The reaction mixture was stirred with a magnetic stirrer to prevent settling of the catalyst. All materials used in the experiments were autoclaved at 121°C for 20 min to ensure sterility. Bacterial suspensions without any antimicrobial materials or with only the SBA-15 support were used as controls. At time intervals of 5, 10, 20, 30 and 60 min after Ag/SBA-15 addition, 0·5 ml of the bacterial suspension was withdrawn and immediately diluted 10-fold in series with 4·5 ml of 0·9% saline solution and plated on LB agar (Fluka Co. 61746) plates. Viable cell counts were determined visually as the number of colonies per plate in serial 10-fold dilutions after incubation at 37°C for 24 h. The reaction temperature was maintained at 25°C.

Inhibition zone tests were carried out on solid agar plates partially covered by filter papers with and without Ag/SBA-15. The solid agar plate with a diameter of 90 mm was prepared by mixing nutrient agar and *E. coli* suspension. The Ag/SBA-15 suspension was dropped on a circle of filter paper with a diameter of 5 mm and dried for 10 min in air. The quantity of Ag/SBA-15 loaded on each filter paper was 1 mg. After the solid agar plates carrying the filter papers were incubated at 37°C for 24 h, the diameter of the inhibition zone was measured with a vernier calliper to estimate the inhibition property of SBA-15.

Reactive oxygen species detection

To determine the production of intracellular ROS, 2′,7′-dichlorofluorescin-diacetate (DCFH-DA, Sigma-Aldrich) was used (Su *et al.* 2009). The *E. coli* samples were collected after centrifugation from LB agar and washed with phosphate-buffered saline (PBS) solution. The *E. coli* samples were then stained with 10 μmol l^{-1} DCFH-DA for 30 min. After that, *E. coli* samples were treated with Ag/SBA-15 and SBA-15 in water separately. Cells stained with DCFH-DA served as the negative control, and H_2O_2 was used as the positive control. Relative fluorescence intensity was recorded using a fluorescent plate reader (Thermo Fisher, Shanghai, China) at an excitation wavelength of 485 nm and emission was measured at a wavelength of 530 nm. Fluorescence intensity was assayed, which was proportional to intracellular ROS concentration. The formation of highly fluorescent DCF was also estimated with a fluorescent microscope (Carl Zeiss Scope A1, Shanghai, China).

Analysis of morphological and structural change

The TEM measurements were used to provide insight into the size, structure and morphology of *E. coli*. To avoid possible damage caused by specimen preparation, native *E. coli* or a suspension of a treated sample was fixed with 2·5% glutaraldehyde, dehydrated by successive soakings in 50, 70, 90 and 100% ethanol and dropped onto copper grids with perforated carbon film. The samples were allowed to dry in air at ambient temperature and were examined using a Hitachi H-7500 electron microscope (Tokyo, Japan) operated at a 80-kV accelerating voltage.

Propidium iodide (PI) was used to examine the disruption of cellular membranes because PI can only influx into cells with disrupted membranes. The staining protocol was as proposed by the manufacturer. Bacteria were first treated with Ag/SBA-15 and SBA-15 in water. The substrates were then washed with PBS and stained with PI dye and subsequently analysed with a fluorescent microscope (Zeiss Scope A1).

Quantitative analysis of potassium, silver ions, nucleic acid and protein

To investigate changes in K^+ concentration during the inactivation of *E. coli*, 5 ml of treated suspension was

withdrawn and filtered through a Millipore filter (pore size 0·22 μm) at each time interval for inductively coupled plasma atomic emission spectroscopy (ICP-AES) on an Optima 2000 (Perkin–Elmer Co., Waltham, MA, USA). All solutions were prepared with ultrapure water. Quantitative analysis of silver ions eluted from antimicrobial materials in treated suspensions was carried out in the same way. To assay cell membrane damage, nucleic acid and protein contents of suspension were directly measured by absorbance at 260 and 280 nm, respectively, using a NanoDrop 2000 spectrometer (Thermo Scientific NanoDrop Technologies, Shanghai, China) after the suspension was centrifuged at 3223 ***g*** for 10 min. All experiments were repeated three times.

Data analysis

All trials were repeated three times. Microbial counts were expressed as log CFU ml^{-1}. The reported data are the mean values of three trials ± standard deviation.

Results

Characterization of Ag/SBA-15

The pore structure of mesoporous samples was investigated by N_2 adsorption/desorption isotherms. Table 1 gives the surface areas, pore diameters and pore volumes of SBA-15 and 1 wt% Ag/SBA-15 samples prepared by the three synthesis methods. As expected, the surface area of SBA-15 decreased after Ag was loaded. The sequence of surface areas was in accordance with the micropore volume (V_{micro}), with SBA-15 > Ag/SBA-15(IWI) > Ag/SBA-15(I) > Ag/SBA-15(DHS). The mesopore volume (V_{meso}) of SBA-15 was the highest, and V_{meso} of Ag/SBA-15(IWI) was the lowest. These results indicated that incipient wetness impregnation mainly induced the blockage of mesoporous pores with Ag particles. However, impregnation and direct hydrothermal synthesis predominately led to blockage of microporous pores during the preparation processes. Furthermore, the largest decrease in V_{meso} and smallest decrease in surface area observed with Ag/SBA-15(IWI) also confirmed that Ag particles were mostly loaded into the mesoporous pores of Ag/SBA-15(IWI).

Figure 1 presents the morphologies of SBA-15 and 1 wt% Ag/SBA-15 samples. In Fig. 1(b), 1 wt% Ag/SBA-15(IWI) presented a regular columnar shape in comparison with the original SBA-15 shown in Fig. 1(a). The surface of 1 wt% Ag/SBA-15(I) was somewhat disordered, and the surface of 1 wt% Ag/SBA-15(DHS) was the most disordered. These results suggest that the morphologies of Ag/SBA-15 were strongly related to the preparation methods.

The TEM images (Fig. 2) show the channel-like pore structure of SBA-15 as well as the framework of Ag/SBA-15 mesoporous materials. The pore channels of SBA-15 were quite uniform, regular and ordered (Fig. 2a). Obviously, incipient wetness impregnation resulted in Ag being confined in the inner walls of SBA-15, which corresponded to the data of Table 1. Since the density of Ag is much higher than that of SiO_2, Ag should be visible in transmission electron micrographs as particles inside pores with high contrast. As a result, the dark particles observed corresponded to Ag particles. The size of particles in the mesopores was about 2–5 nm. By contrast, most Ag particles were spread on the surfaces of Ag/SBA-15(I) and Ag/SBA-15(DHS) with sizes between 10–30 nm.

Antimicrobial activity of Ag/SBA-15

To test the antimicrobial activity of Ag/SBA-15, inhibition zone and bactericidal activity measurements were performed. Figure 3(a) shows the images of bacteriological tests performed on solid agar plates partially covered by filter papers with and without Ag/SBA-15. In the case of 1 wt% Ag/SBA-15, an inhibition zone formed with a diameter of about 10 mm, indicating that Ag/SBA-15 clearly restrained the proliferation of *E. coli*. By comparison, no inhibition zone appeared around the blank filter paper ($0^{\#}$) and filter paper treated with SBA-15 ($1^{\#}$).

The bactericidal activity of 1 wt% Ag/SBA-15 in water at room temperature was investigated. With SBA-15 addition, a 1·5 log decrease in survival was observed after 60 min. However, in the presence of 1 wt% Ag/SBA-15 (IWI), there was 4·5 log decrease in *E. coli* in survival for 60 min. In addition, 1 wt% Ag/SBA-15(I) and (DHS) could result in 7·5 log inactivation for 60 min (Fig. 3b). Ag/SBA-15 samples were so effective that the surviving

Table 1 Surface areas and porous properties of SBA-15 and Ag/SBA-15

Samples	Surface area (m^2 g^{-1})	Pore diameter (nm)	Pore volume (cm^3 g^{-1})	V_{micro} (cm^3 g^{-1})	V_{meso} (cm^3 g^{-1})
SBA-15	885·2	4·65	1·03	0·17	0·95
Ag/SBA-15(IWI)	749·9	4·66	0·83	0·16	0·75
Ag/SBA-15(I)	629·8	5·56	0·93	0·06	0·90
Ag/SBA-15(DHS)	571·9	6·13	0·89	0	0·89

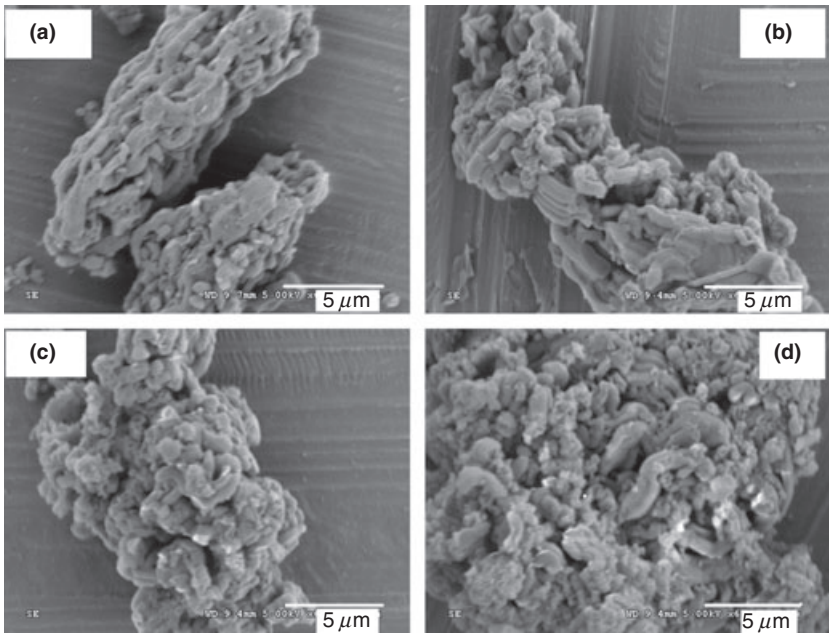

Figure 1 SEM images of (a) SBA-15, (b) 1 wt % Ag/SBA-15(IWI), (c) 1 wt% Ag/SBA-15(I) and (d) 1 wt% Ag/SBA-15(DHS).

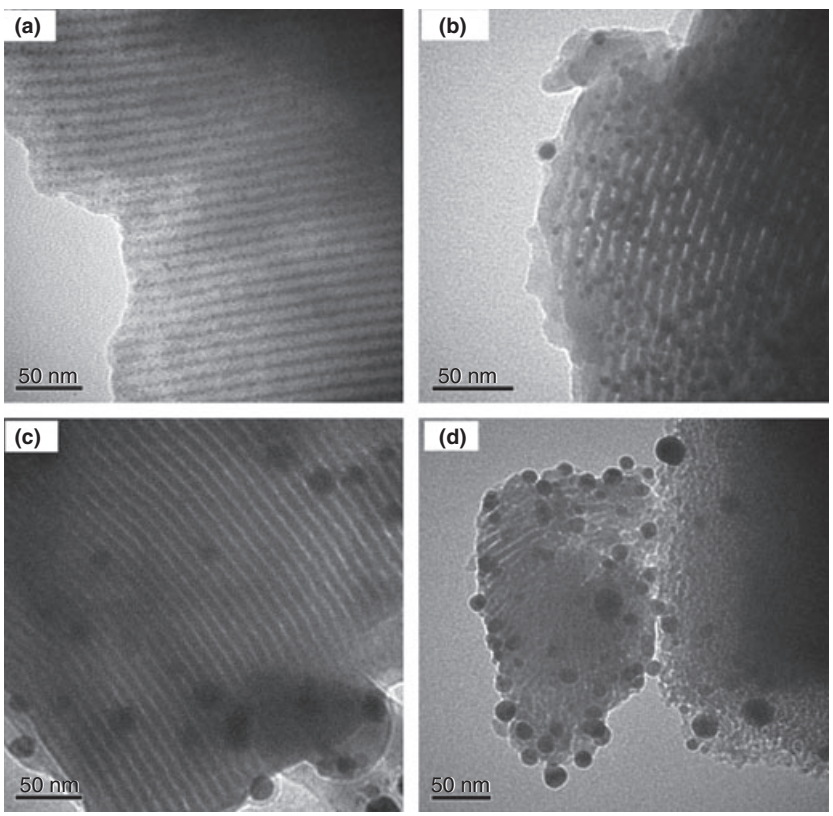

Figure 2 TEM images of (a) SBA-15, (b) 1 wt % Ag/SBA-15(IWI), (c) 1 wt% Ag/SBA-15(I) and (d) 1 wt% Ag/SBA-15(DHS).

E. coli cells decreased sharply even in the first 10 min. In addition, the minimum inhibitory concentration (MIC) and minimum bactericidal concentration (MBC) of 1 wt % Ag/SBA-15 (IWI) were 15 and 25 mg l^{-1}, respectively. 1 wt% Ag/SBA-15(I) and (DHS) had the same MIC values of 10 mg l^{-1} and the same MBC values of 15 mg l^{-1}.

Table 2 gives the survival changes of *E. coli* in the presence of different samples loaded with different amounts

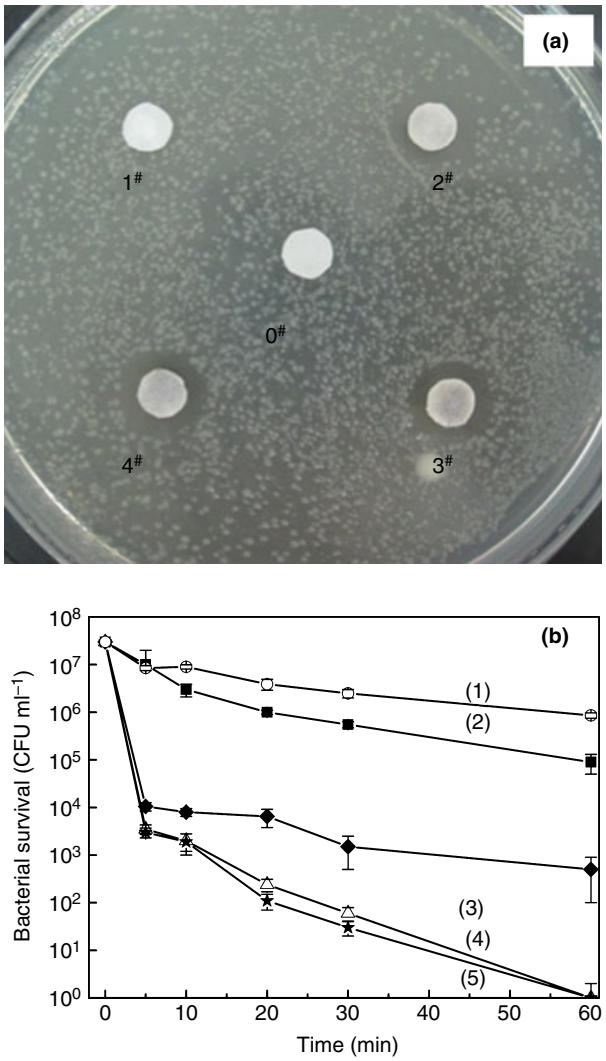

Figure 3 (a) Images of *Escherichia coli* incubated for 24 h at 37°C together with blank filter paper (0#), and filter papers treated with 1 mg SBA-15 (1#), 1 wt% Ag/SBA-15(IWI) (2#), 1 wt% Ag/SBA-15(I) (3#) and 1 wt% Ag/SBA-15(DHS) (4#). Initial bacterial count: 1×10^5 CFU. (b) Bactericidal activity of (1) SBA-15, (2) 0·5 mg l^{-1} Ag^+, (3) 1 wt% Ag/SBA-15(IWI), (4) 1 wt% Ag/SBA-15(I) and (5) 1 wt% Ag/SBA-15(DHS) against *E. coli* at room temperature: sample concentration, 50 mg l^{-1}; initial bacterial concentration, 3×10^7 CFU ml^{-1}.

of silver as well as with SBA-15 used as a control. Bactericidal activity was clearly enhanced with the increase in the amount of silver. It only took 20 and 30 min for complete inactivation of *E. coli* with 4 wt% Ag/SBA-15 (DHS) and Ag/SBA-15(I), respectively. The 0·5 wt% Ag/SBA-15 also induced a 4–5 log unit reduction in viable cells, which revealed that even a low amount of silver exhibited high bactericidal activity. For the control, with SBA-15 addition, viable cell count was reduced by a 1·0 log unit after 30 min, probably because of the adsorption function of the support. This means that the dramatic decrease in *E. coli* survival was mainly due to the highly efficient bactericidal activity of Ag/SBA-15. These results indicate that Ag/SBA-15 was a promising material for antimicrobial application with high antimicrobial activity.

Effect of Ag^+ and ROS in bactericidal process

To clarify whether the Ag^+ eluted from Ag/SBA-15 was the dominant factor responsible for the bactericidal activity, a quantitative analysis of Ag^+ eluted from the material into deionized water was performed using ICP-AES. The eluted Ag^+ concentrations measured for various specimens after different periods in water with vigorous stirring are shown in Table 3. As shown from Table 3, the concentration of Ag^+ eluted from Ag/SBA-15 (IWI) was only 0·039 mg l^{-1} within 120 min. However, after 120 min, the amounts of Ag^+ eluted from Ag/SBA-15 (I) and (DHS) were 0·275 and 0·498 mg l^{-1}, respectively. It is worth noting that the amount of Ag^+ eluted from Ag/SBA-15(IWI) was much less than that from Ag/SBA-15(I) and (DHS), indicating that incipient wetness impregnation largely reduced the speed of silver elution and decreased the potential health risk to human beings. The maximum permissible concentration level of Ag^+ in drinking water is 0·09 mg l^{-1}, as declared by the World Health Organization (WHO) (Sökmen *et al.* 2001; Zhang *et al.* 2003). The obvious decrease in the release rate of Ag^+ might be due to the slow diffusion in mesopores. Furthermore, at a concentration of 0·5 mg l^{-1}, Ag^+ showed low bactericidal activity within 60 min (Fig. 3b), while the concentration of Ag^+ eluted from all Ag/SBA-15 materials was less than 0·5 mg l^{-1} within 120 min. These results clearly suggest that the toxicity of Ag^+ in solution was not fully responsible for the inactivation of *E. coli* by Ag/SBA-15. Considering that Ag/SBA-15, as an oxidative catalyst (Tian *et al.* 2009), should have the capacity to transform O_2 into ROS that might contain superoxide anions ($^{\cdot}O_2^-$), hydrogen peroxide (H_2O_2) and hydroxyl radicals ($^{\cdot}OH$), we supposed that ROS catalytically formed by the catalyst might also contribute to the bactericidal effect of Ag/SBA-15 during the bactericidal process. The differences in bactericidal activities among Ag/SBA-15(IWI), (I) and (DHS) shown in Fig. 3(b) might be due to the different concentrations of Ag^+ eluted and the different amounts of ROS that could diffuse and come into contact with *E. coli*. In the following experiments, ROS scavengers were added to clarify the effect of extracellular ROS on bactericidal activity.

In this experiment, 200 units ml^{-1} superoxide dismutase (SOD), 175 units ml^{-1} catalase and 0·3 mol l^{-1} methanol were used as scavengers for the superoxide anions $^{\cdot}O_2^-$, H_2O_2 and $^{\cdot}OH$, respectively. The effect of ROS scavengers on the bactericidal activity of 1 wt% Ag/

Table 2 Bactericidal activity of Ag/SBA-15 samples loaded with different amounts of silver against *Escherichia coli* at room temperature

Samples (50 mg l^{-1})	Content of Ag	Time (min)				
		0	5	10	20	30
SBA-15	0	(1·5 ± 0·5) *10^7	(9·0 ± 1·0) *10^6	(1·2 ± 0·7) *10^6	(1·0 ± 0·4) *10^6	(9·0 ± 2·4) *10^5
Ag/SBA-15 (ISI), wt%	0·5	(1·5 ± 0·5) *10^7	(3·1 ± 1·6) *10^4	(2·9 ± 1·7) *10^4	(8·8 ± 2·7) *10^3	(5·0 ± 2·1) *10^3
	1	(1·5 ± 0·5) *10^7	(1·1 ± 1·2) *10^4	(7·9 ± 1·9) *10^3	(6·2 ± 1·9) *10^3	(1·5 ± 0·8) *10^3
	2	(1·5 ± 0·5) *10^7	(8·6 ± 1·1) *10^3	(4·9 ± 2·3) *10^3	(3·2 ± 1·3) *10^3	(1·0 ± 0·6) *10^3
	4	(1·5 ± 0·5) *10^7	(3·7 ± 2·1) *10^3	(3·0 ± 1·4) *10^3	(1·6 ± 0·7) *10^3	(2·7 ± 3·2) *10^2
	6	(1·5 ± 0·5) *10^7	(1·0 ± 0·9) *10^3	(5·8 ± 2·2) *10^2	(3·8 ± 1·2) *10^2	(4·0 ± 1·4) *10^1
Ag/SBA-15 (I), wt%	0·5	(1·5 ± 0·5) *10^7	(8·9 ± 1·5) *10^3	(4·3 ± 1·5) *10^3	(1·5 ± 0·6) *10^3	(3·9 ± 0·7) *10^2
	1	(1·5 ± 0·5) *10^7	(3·4 ± 1·2) *10^3	(2·0 ± 1·5) *10^3	(2·3 ± 0·9) *10^2	(6·0 ± 2·5) *10^1
	2	(1·5 ± 0·5) *10^7	(1·8 ± 0·8) *10^3	(2·2 ± 2·0) *10^3	(1·8 ± 1·5) *10^2	(1·2 ± 0·5) *10^2
	4	(1·5 ± 0·5) *10^7	(1·2 ± 0·9) *10^3	(8·3 ± 2·5) *10^2	(4·6 ± 3·0) *10^1	–*
	6	(1·5 ± 0·5) *10^7	(9·0 ± 2·7) *10^2	(7·0 ± 3·0) *10^2	(2·6 ± 2·5) *10^1	–*
Ag/SBA-15 (DHS), wt%	0·5	(1·5 ± 0·5) *10^7	(7·0 ± 1·8) *10^3	(8·1 ± 2·3) *10^3	(2·0 ± 1·7) *10^3	(4·1 ± 1·3) *10^2
	1	(1·5 ± 0·5) *10^7	(3·0 ± 1·4) *10^3	(2·3 ± 1·6) *10^3	(1·2 ± 0·5) *10^2	(3·0 ± 2·2) *10^1
	2	(1·5 ± 0·5) *10^7	(1·1 ± 0·9) *10^3	(8·8 ± 2·4) *10^2	(7·6 ± 1·8) *10^2	(4·0 ± 0·8) *10^1
	4	(1·5 ± 0·5) *10^7	(8·0 ± 2·6) *10^2	(6·5 ± 2·1) *10^1	–*	–*
	6	(1·5 ± 0·5) *10^7	(5·5 ± 3·4) *10^1	(2·3 ± 1·6) *10^1	–*	–*

*No available cells.

Table 3 Concentration of eluted Ag^+ from Ag/SBA-15 samples and leakage of K^+, nucleic acid and protein from *Escherichia coli* cells in the presence of SBA-15 and Ag/SBA-15

50 mg l^{-1}	Concentration of eluted Ag^+ (mg l^{-1})			K^+ leakage (mg l^{-1})			Leakage of nucleic acid (ng μl^{-1})	Leakage of protein (μg ml^{-1})
	10 min	30 min	120 min	10 min	30 min	60 min	30 min	30 min
SBA-15				0·092	0·105	0·117	1·1	13
1 wt% Ag/SBA-15 (IWI)	0·006	0·021	0·039	0·160	0·215	0·238	2·4	53
1 wt% Ag/SBA-15 (I)	0·231	0·298	0·275	0·194	0·223	0·259	3·0	29
1 wt% Ag/SBA-15 (DHS)	0·209	0·464	0·498	0·190	0·236	0·265	5·1	36

SBA-15(IWI) is shown in Fig. 4. The bactericidal effect was weakened by the addition of catalase or methanol, compared with the control experiment without any ROS scavengers, at corresponding time intervals. When two scavengers (SOD and catalase) were introduced together, the bactericidal effect decreased further. These results suggest the formation of $^{\cdot}O_2^-$, H_2O_2 and $^{\cdot}OH$ on the Ag/SBA-15(IWI) surface and their contribution to the bactericidal effect. As previously reported, transition metals such as silver can catalyse H_2O_2, resulting in the formation of $^{\cdot}OH$ (Inoue *et al.* 2002; Pape *et al.* 2004). Furthermore, to exclude the effect of Ag^+ existing on the surface or in mesopores of catalysts as well as dissociated Ag^+, bactericidal activity was examined in physiological saline. The bactericidal activity noticeably decreased in physiological saline compared with that in deionized water. The effect of physiological saline was higher than the toxicity of Ag^+ alone (Fig. 3b), indicating that Ag^+ on the surface or in the mesopores of the catalyst played a catalytic role because the redox process of Ag^0/Ag^+ usually contributes to the formation of ROS through Fenton-like reactions. The growth curve of *E. coli* in water was the same as that in 0·9% NaCl with no addition of Ag/SBA-15. Thus, the bactericidal effect of Ag/SBA-15 was a synergistic action of extracellular ROS and Ag^+. Similar phenomena were found in the bactericidal processes of Ag/SBA-15(I) and (DHS) (not shown).

To examine the effect of ROS induced by Ag/SBA-15 materials on *E. coli* cells *in vivo*, DCFH-DA was used as an intracellular ROS indicator for the Ag/SBA-15 treated cells to measure the generation of intracellular ROS (Su *et al.* 2009). Figure 5(a) shows that after Ag/SBA-15 treatment, *E. coli* cells became DCF positive, indicating that intracellular ROS were generated and participated in the Ag/SBA-15-induced cell death. In contrast, only a few cells became DCF positive with SBA-15 treatment. For comparison, relative fluorescence intensity (i.e. relative ROS level) is presented in Fig. 5(b). Cells treated with Ag/SBA-15 (DHS) displayed the highest relative ROS level, which was consistent with the order of

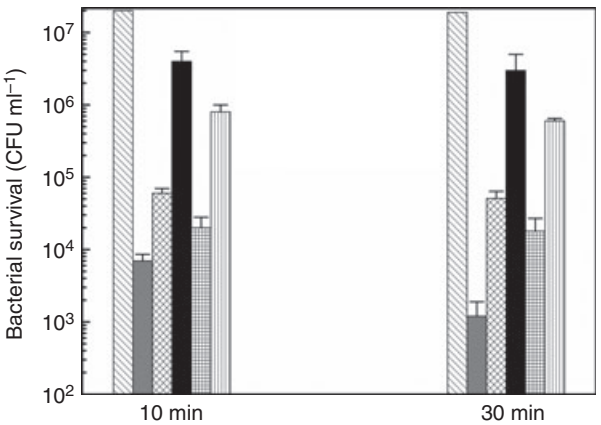

Figure 4 Effect of ROS scavengers on bactericidal activity of 1 wt% Ag/SBA-15(IWI). (▨) Control; (▩) Ag/SBA-15; (▩) Ag/SBA-15 + catalase; (■) Ag/SBA-15 + catalase+SOD; (▩) Ag/SBA-15 + CH_3OH and (▩) Ag/SBA-15 + physiological saline.

antimicrobial activity. Cells treated with 0·5 mg l^{-1} Ag^+ also had a higher relative ROS level than those treated with SBA-15 and lower than those treated with Ag/SBA-15. These results suggest that intracellular ROS, induced by extracellular ROS and Ag^+, was a candidate mediator for the cell apoptosis and death.

Morphological and structural change and K^+, nucleic acid, protein leakage

After Ag/SBA-15 (IWI) treatment, TEM micrographs revealed dramatic changes in the nature of the contents of cells and in the structure of the cell walls, as shown in Fig. 6(b) and (c). Compared with the normal cells shown in Fig. 6(a), the cells were no longer uniform following cell wall disruption, leakage of intracellular constituents leading to small protuberances (indicated by arrows) and condensation of cell cytoplasm. The cytoplasmic membrane of some cells shrank and became detached from the cell wall (indicated by double-arrow) (Fig. 6b,d), which might be attributable to the interaction between Ag^+ and thiol groups in cytoplasmic protein (Feng *et al.* 2000). Chang *et al.* (2008a,b) previously observed the same phenomenon after treatment with 1 mg l^{-1} Ag^+. Furthermore, the different morphological changes in *E. coli* cells treated with Ag/SBA-15 (IWI) and those treated with Ag^+ implied that two different antimicrobial mechanisms were involved. The formation of extracellular ROS was active in destroying the cells.

The membrane integrity of the cells was reflected by the influx of membrane-impermeable fluorescent PI since PI can only influx into cells with disrupted membranes. Figure 7 shows that the number of PI-positive cells treated with Ag/SBA-15 was obviously higher than that of PI-positive cells treated with SBA-15 only. These results suggest that the antimicrobial ability of Ag/SBA-15 involved the disruption of membrane integrity through the generation of intracellular ROS.

The outer cell membrane plays an essential role in providing a barrier of selective permeability for *E. coli* and other Gram-negative bacteria (Amro *et al.* 2000). On the basis of the TEM investigation and PI-positive results, after treatment with Ag/SBA-15 (IWI), (I) and (DHS), the cell wall and cell membrane were destroyed, which might lead to a change in cell membrane permeability and leakage of intracellular substances. K^+ exists universally in bacteria (Heefner 1982; Lu *et al.* 2003) and plays an important role in the regulation of polysome content and protein synthesis. The release of intracellular protein and nucleic acid is also an important indicator of cell membrane damage (Woo *et al.* 2000; Hong *et al.* 2004). Therefore, leakage of K^+, nucleic acid and protein from *E. coli* cells was used to further examine the permeability and damage of the cell membrane. Table 3 shows the changes in K^+, nucleic acid and protein concentrations in the presence of various 1 wt% Ag/SBA-15 samples, with SBA-15 as the control. In the case of the SBA-15 control, there was almost 0·1 mg l^{-1} of K^+ leakage from *E. coli* cells, and the amount of K^+ had no observable increase for 60 min. In the presence of Ag/SBA-15, however, about 0·2 mg l^{-1} of K^+ leaked from the bacterial cells just 10 min after the addition of samples, which should be attributed to a notable change in the structure of the outer membrane. The K^+ concentration increased with increasing time and reached relatively steady values after 60 min, when nearly 100% cell inactivation was achieved. Nucleic acid and its related compounds, such as pyrimidines and purines, were detected using a NanoDrop spectrometer. The leakage concentration of nucleic acid of cells treated with 1 wt% Ag/SBA-15 was 2–5 times higher than the 1·1 ng μl^{-1} of the control suspension. Furthermore, the release of intracellular proteins was also found in suspension for injured cells. The amount of protein released into the treated cell suspension was much higher than that released into the control suspension. The presence of these intracellular contents in suspension indicated severe damage to cells at the membrane level. The cell wall and membrane damage was achieved through intracellular ROS induced by extracellular ROS with strongly oxidizing properties and Ag^+.

Discussion

Among different antimicrobial agents, silver has high antimicrobial activity and has been used widely. However, materials including silver usually have high costs. In addition, the elution of Ag^+ when silver is used for water

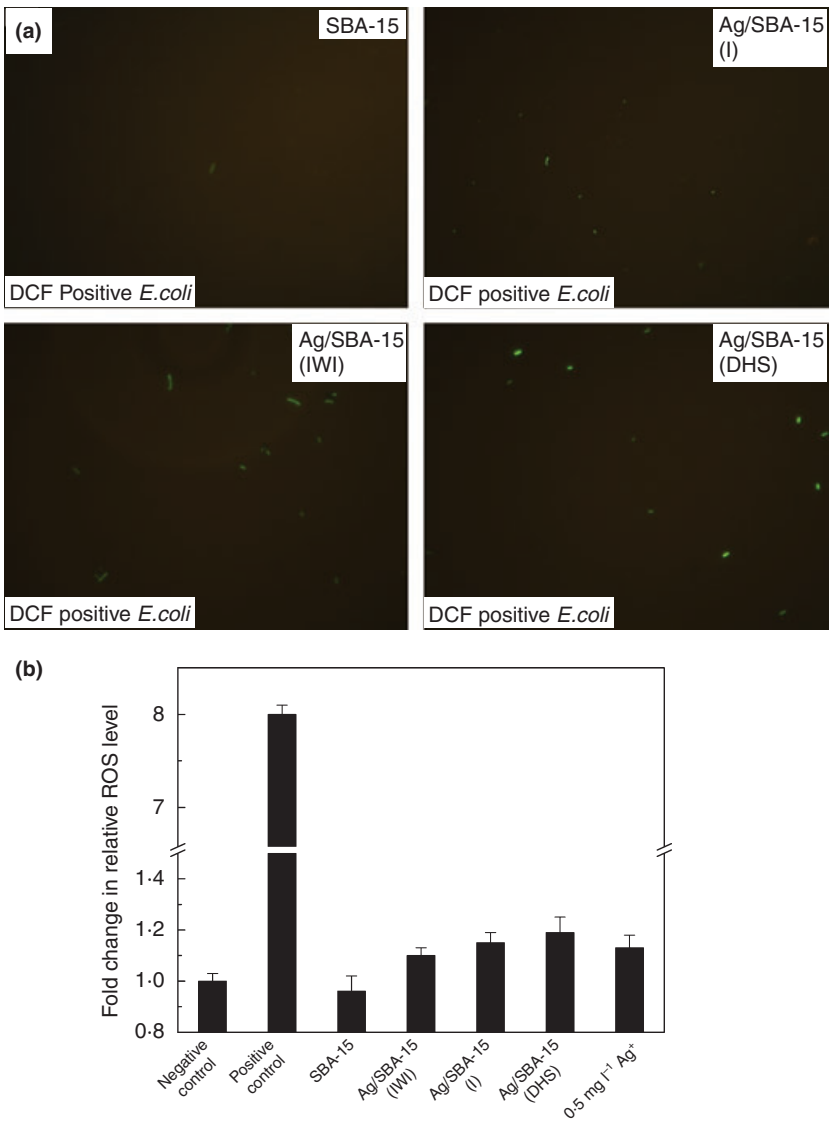

Figure 5 Ag/SBA-15-induced ROS production in *Escherichia coli* cells. (a) The photographs of fluorescence microscope of *E. coli* treated with SBA-15 and 1 wt% Ag/SBA-15 samples for 1 h separately after stained with 10 μmol l^{-1} DCFH-DA. (b) The average of fluorescence intensities in each group was expressed. The cells with DCFH-DA labelling served as negative control, and H_2O_2 was used as positive control. 0·5 mg l^{-1} Ag^+ was used as another control. Sample concentration, 50 mg l^{-1}; initial bacterial concentration, 1×10^7 CFU ml^{-1}.

disinfection is of concern for human health. Our results showed that Ag/SBA-15 possessed high antimicrobial activities with the addition of only a small amount of silver, thus reducing the usual associated costs. The amount of Ag^+ eluted from Ag/SBA-15 prepared by incipient wetness impregnation was lower than the maximum permissible concentration level of 0·09 mg l^{-1} Ag^+ in drinking water declared by the WHO. Therefore, Ag/SBA-15 material shows potential advantages for use as antimicrobial material.

Silver, especially in nanoscale form, has strong biological effects against micro-organisms. The silver loaded onto the surface or in the inner wall of SBA-15 were nanoscale particles (Fig. 2). Such metal nanoparticles interact with microbial cells through multiple biochemical pathways, for instance, via Ag^+ and the production of ROS (Marambio-Jones and Hoek 2010). ROS can damage cell structures and ultimately cause cell death (Neal 2008; Su *et al.* 2009). It is well known that Ag^+ in high concentrations exhibits bactericidal activity (Feng *et al.* 2000; Matsumura *et al.* 2003), and Ag^+ elution from Ag-loaded materials cannot be avoided under the experimental conditions. Lalueza *et al.* (2011) reported that 1·5 mg l^{-1} of silver nitrate did not show significant antimicrobial effects. Our results also showed that at a concentration of 0·5 mg l^{-1}, Ag^+ showed low bactericidal activity. In this study, Ag^+ concentration was lower than the 0·5 mg l^{-1} eluted from each Ag/SBA-15 catalyst prepared with different methods, which indicated that the antimicrobial activity did not depend on the toxicity of silver ions only.

Experimental results indicated that silver loaded on SBA-15 also involved extracellular and intracellular ROS

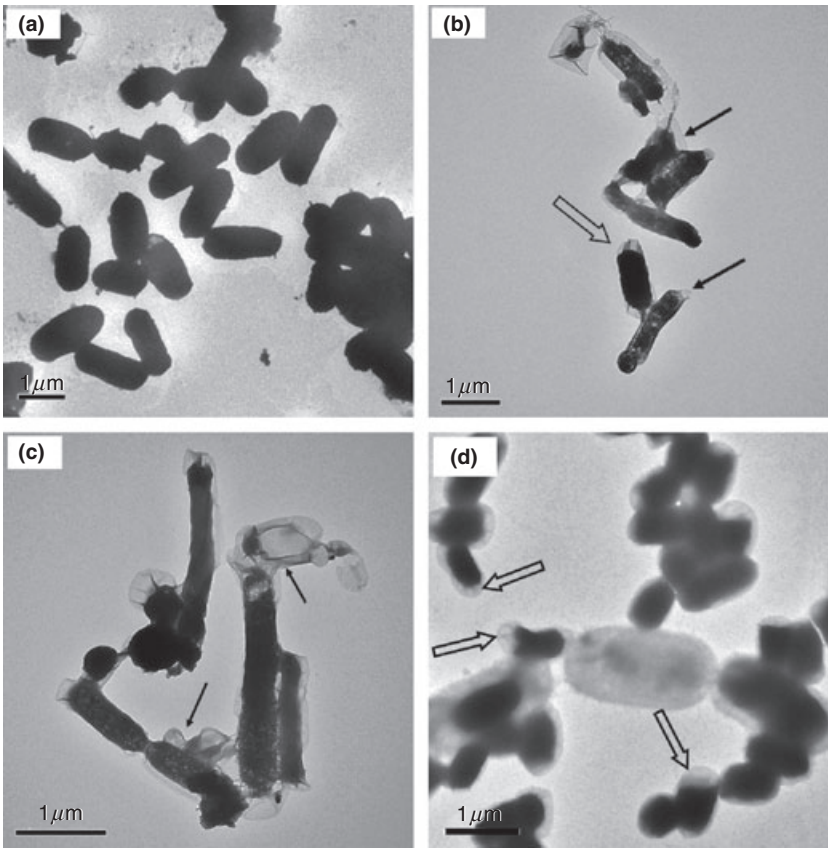

Figure 6 TEM images of (a) untreated *Escherichia coli* cells in water for 1 h and *E. coli* cells treated with (b) 1 wt% Ag/SBA-15(IWI) in water for 30 min, (c) 1 wt% Ag/SBA-15(IWI) and (d) 0·5 mg l^{-1} Ag^{+} for 1 h at room temperature.

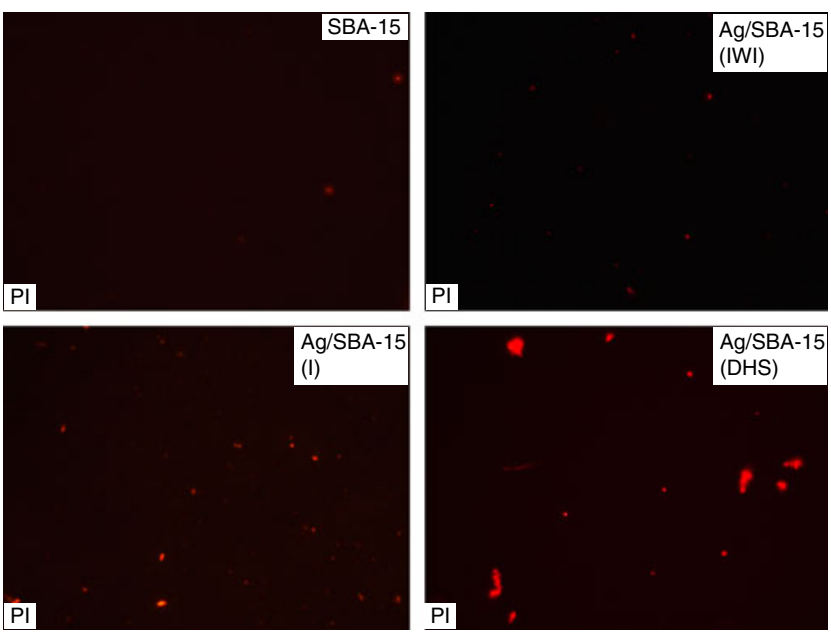

Figure 7 Ag/SBA-15-induced membranes disruption of *Escherichia coli* cells. The photographs of fluorescence microscope of *E. coli* treated with SBA-15 and 1 wt% Ag/SBA-15 samples for 1 h respectively, where dead cells were positive for PI (red). Sample concentration, 50 mg l^{-1}; initial bacterial concentration, 1·5 × 10^{7} CFU ml^{-1}.

roles in the process of cell death. The addition of SOD, catalase and methanol proved the production of extracellular ROS. When Ag was dispersed as metal particles on some oxides, the Ag particle surface might have sufficient defects for dissociative chemisorption of oxygen (Bera *et al.* 1999, 2000). Therefore, it was believed that the redox cycle of Ag^{+}/Ag^{0} maintained the catalytic process of extracellular ROS formation. Furthermore, Ag^{+} might

be helpful for the production of extracellular ROS according to the Fenton-like mechanism. Importantly, extracellular ROS induced intracellular ROS production and death of cells. Moreover, Ag^+ also aided in the generation of intracellular ROS, which were produced through respiratory enzymes by Ag^+ (Matsumura *et al.* 2003). This was proved by the appearance of DCF-positive cells treated with 0·5 mg l^{-1} Ag^+ (Fig. 5). In all, the catalytically antimicrobial effect should be considered as a synergic action of extracellular ROS and Ag^+. Intracellular ROS was the candidate mediator for the death of cells involved in the Ag/SBA-15 antimicrobial system.

Furthermore, physiological disturbances such as electron transport and respiration might occur in the Ag/SBA-15 system like the effects of many metals. Bacteria were cytostatic when in contact with AgNP/Clay, implying that the motor function of the cytoskeletons was hampered (Su *et al.* 2009). Previous research also indicated that silver nanoparticles affected membrane receptor internalization and cellular signalling and protein expression (Jiang *et al.* 2008). Yamanaka *et al.* (2005) confirmed that silver ions could penetrate cells and affect ribosomal subunit proteins and some enzymes important for bacterial cells. Furthermore, owing to the membrane damage caused by silver nanoparticles, cells cannot effectively extrude Ag^+ and restrict their effect (Hwang *et al.* 2008). According to the literature and production of intracellular ROS, some Ag/SBA-15 particles that contacted with cells might have disturbed normal physiological function of membrane proteins, such as channels or receptors, and consequently interfered with the proton pool in the membrane space or the electronic flow through the respiratory chain. Accumulated electrons could be transferred to oxygen to form intracellular ROS, leading to oxidative damage and membrane leakage in bacteria.

In conclusion, Ag/SBA-15 exhibited good antimicrobial activity against *E. coli* cells at room temperature. The silver species strongly enhanced the antimicrobial activity of the samples by catalysing the reaction of adsorbed O_2 to form extracellular ROS, such as $^{\cdot}O_2^-$, H_2O_2 and $^{\cdot}OH$. The antimicrobial effect was a synergistic action of extracellular ROS and toxicity of Ag^+, which induced the production of intracellular ROS and death of cells. With strong oxidizing properties, ROS resulted in the destruction of the cell wall and cell membrane of *E. coli*, leading to leakage of intracellular components such as K^+, nucleic acid and protein. Considering the low amount of Ag^+ elution, the Ag/SBA-15(IWI) mesoporous material prepared by incipient wetness impregnation was the most promising antimicrobial technology application for drinking water treatment. Further work on the antimicrobial activities of these materials against Gram-positive bacteria and fungus is still required.

Acknowledgements

This work was financially supported by the National Natural Science Foundation of China (No. 51208497) and the National High Technology Research and Development Program of China (No. 2010AA064905, 2012AA 062702).

Conflict of Interest

The authors declare no conflict of interest.

References

Amro, N.A., Kotra, L.P., Kapila, W.M., Bulychev, A., Mobashery, S. and Liu, G. (2000) High-resolution atomic force microscopy studies of the *Escherichia coli* outer membrane: structural basis for permeability. *Langmuir* **16**, 2789–2796.

Bera, P., Patil, K.C., Jayaram, V., Hegde, M.S. and Subbanna, G.N. (1999) Combustion synthesis of nanometal particles supported on α-Al_2O_3: CO oxidation and NO reduction catalysts. *J Mater Chem* **9**, 1801–1805.

Bera, P., Patil, K.C. and Hegde, M.S. (2000) NO reduction, CO and hydrocarbon oxidation over combustion synthesized Ag/CeO_2 catalyst. *Phys Chem Chem Phys* **2**, 3715–3719.

Cai, X.H., Zhu, G.S., Gao, B. and Zhang, W.W. (2006) Preparation of Ag/SBA-15 nanocomposite and its bactericidal activity. *Chem J Chin Univ* **27**, 2042–2044.

Chamakura, K., Perez-Ballestero, R., Luo, Z.P., Bashir, S. and Liu, J.B. (2011) Comparison of bactericidal activities of silver nanoparticles with common chemical disinfectants. *Colloids Surf B Biointerfaces* **84**, 88–96.

Chang, Q.Y., Yan, L.Z., Chen, M.X., He, H. and Qu, J.H. (2007) Bactericidal mechanism of Ag/Al_2O_3 to *E. coli*. *Langmuir* **23**, 11197–11199.

Chang, Q.Y., He, H., Zhao, J.C., Yang, M. and Qu, J.H. (2008a) Bactericidal activity of a Ce-Promoted Ag/$AlPO_4$ catalyst using molecular oxygen in water. *Environ Sci Technol* **42**, 1699–1704.

Chang, Q.Y., He, H. and Ma, Z.C. (2008b) Efficient disinfection of *Escherichia coli* in water by silver loaded alumina. *J Inorg Biochem* **102**, 1736–1742.

Chen, M.X., Yan, L.Z., He, H., Chang, Q.Y., Yu, Y.B. and Qu, J.H. (2007) Catalytic sterilization of *Escherichia coli* K 12 on Ag/Al_2O_3 surface. *J Inorg Biochem* **101**, 817–823.

Dollimore, D. and Heal, G.R. (1964) An improved method for the calculation of pore size distribution from adsorption data. *J Appl Chem* **14**, 109–114.

Feng, Q.L., Wu, J., Chen, G.Q., Cui, F.Z., Kim, T.N. and Kim, J.O.A. (2000) A mechanistic study of the antibacterial effect of silver ions on *Escherichia coli* and *Staphylococcus aureus*. *J Biomed Mater Res* **52**, 662–668.

He, H., Dong, X.P., Yang, M., Yang, Q.X., Duan, S., Yu, Y.B., Han, J., Zhang, C.B. *et al.* (2004) Catalytic inactivation of SARS coronavirus, *Escherichia coli* and yeast on solid surface. *Catal Commun* **5**, 170–172.

Heefner, D.L. (1982) Transport of H+, K+, Na+ and Ca++ in Streptococcus. *Mol Cell Biochem* **44**, 81–106.

Hong, S.M., Park, J.K. and Lee, Y.O. (2004) Mechanisms of microwave irradiation involved in the destruction of fecal coliforms from biosolids. *Water Res* **38**, 1615–1625.

Hwang, E.T., Lee, J.H., Chae, Y.J., Kim, Y.S., Kim, B.C., Sang, B. and Gu, M.B. (2008) Analysis of the toxic mode of action of silver nanoparticles using stress-specific bioluminescent bacteria. *Small* **4**, 746–750.

Inoue, Y., Hoshino, M., Takahashi, H., Noguchi, T., Murata, T., Kanzaki, Y., Hamashima, H. and Sasatsu, M. (2002) Bactericidal activity of Ag–zeolite mediated by reactive oxygen species under aerated conditions. *J Inorg Biochem* **92**, 37–42.

Ivanova, E.P., Hasan, J., Truong, V.K., Wang, J.Y., Raveggi, M., Fluke, C. and Crawford, R.J. (2011) The influence of nanoscopically thin silver films on bacterial viability and attachment. *Appl Microbiol Biotechnol* **91**, 1149–1157.

Jiang, W., Kim, B.Y., Rutka, J.T. and Chan, W.C. (2008) Nanoparticle-mediated cellular response is size-dependent. *Nat Nanotechnol* **3**, 145–150.

Kawahara, K., Tsuruda, K., Morishita, M. and Uchida, M. (2000) Antibacterial effect of silver-zeolite on oral bacteria under anaerobic conditions. *Dent Mater* **16**, 452–455.

Kim, S.W., Baek, Y.W. and An, Y.J. (2011) Assay-dependent effect of silver nanoparticles to *Escherichia coli* and *Bacillus subtilis*. *Appl Microbiol Biotechnol* **92**, 1045–1052.

Kwakye-Awuah, B., Williams, C., Kenward, M.A. and Radecka, I. (2008) Antimicrobial action and efficiency of silver-loaded zeolite X. *J Appl Microbiol* **104**, 1516–1524.

Lalueza, P., Monzon, M., Arruebo, M. and Santamaria, J. (2011) Bactericidal effects of different silver-containing materials. *Mater Res Bull* **46**, 2070–2076.

Liong, M., France, B., Bradley, K.A. and Zink, J.I. (2009) Antimicrobial activity of silver nanocrystals encapsulated in mesoporous silica nanoparticles. *Adv Mater* **21**, 1–6.

Lippens, B.G. and Boer, J.H. (1965) Studies on pore systems in catalysts: V. The t method. *J Catal* **4**, 319–323.

Lu, Z.X., Zhou, L., Zhang, Z.L., Shi, W.L., Xie, Z.X., Xie, H.Y., Pang, D.W. and Shen, P. (2003) Cell damage induced by photocatalysis of TiO_2 thin films. *Langmuir* **19**, 8765–8768.

Marambio-Jones, C. and Hoek, E.M.V. (2010) A review of the antibacterial effects of silver nanomaterials and potential implications for human health and the environment. *J Nanopart Res* **12**, 1531–1551.

Matsumura, Y., Yoshikata, K., Kunisaki, S.I. and Tsuchido, T. (2003) Mode of bactericidal action of silver zeolite and its comparison with that of silver nitrate. *Appl Environ Microbiol* **69**, 4278–4281.

Neal, A.L. (2008) What can be inferred from bacterium nanoparticle interactions about the potential consequences of environmental exposure to nanoparticles? *Ecotoxicology* **17**, 362–371.

Pape, H.L., Solano-Serena, F., Contini, P., Devillers, C., Maftah, A. and Leprat, P. (2004) Involvement of reactive oxygen species in the bactericidal activity of activated carbon fibre supporting silver bactericidal activity of ACF(Ag) mediated by ROS. *J Inorg Biochem* **98**, 1054–1060.

Rai, M.K., Deshmukh, S.D., Ingle, A.P. and Gade, A.K. (2012) Silver nanoparticles: the powerful nanoweapon against multidrug-resistant bacteria. *J Appl Microbiol* **112**, 841–852.

Sayari, A. (1996) Catalysis by crystalline mesoporous molecular sieves. *Chem Mater* **8**, 1840–1852.

Schacht, V.J., Neumann, L.V., Sandhi, S.K., Chen, L., Henning, T., Klar, P.J., Theophel, K., Schnell, S. *et al.* (2012) Effects of silver nanoparticles on microbial growth dynamics. *J Appl Microbiol* **114**, 25–35.

Sökmen, M., Candan, F. and Sümer, Z. (2001) Disinfection of *E. coli* by the Ag-TiO_2/UV system: lipid peroxidation. *J Photochem Photobiol A Chem* **143**, 241–244.

Sondi, I. and Salopek-Sondi, B. (2004) Silver nanoparticles as antimicrobial agent: a case study on *E. coli* as a model for Gram-negative bacteria. *J Colloid Interface Sci* **275**, 177–182.

Su, H.L., Chou, C.C., Hung, D.J., Lin, S.H., Pao, I.C., Lin, J.H., Huang, F.L., Dong, R.X. *et al.* (2009) The disruption of bacterial membrane integrity through ROS generation induced by nanohybrids of silver and clay. *Biomaterials* **30**, 5979–5987.

Tian, D., Yong, G.P., Dai, Y., Yan, X.Y. and Liu, S.M. (2009) CO oxidation catalyzed by Ag/SBA-15 catalysts prepared via *in situ* reduction: the influence of reducing agents. *Catal Lett* **130**, 211–216.

TIC (1998) Trend of the latest technology judging from Japanese patents: antibacterial and antifungal ceramics (II)/series no. 1014. Osaka.

Wan, Y.Z., Wang, Y.L., Cheng, G.X., Luo, H.L. and Dong, X.H. (2001) Preparation and characterization of activated carbon fiber supporting silver-loaded mesoporous molecular sieves. *Carbon* **39**, 1605–1616.

Woo, I.S., Rhee, I.K. and Park, H.D. (2000) Differential damage in bacterial cells by microwave radiation on the basis of cell wall structure. *Appl Environ Microbiol* **66**, 2243–2247.

Yamanaka, M., Hara, K. and Kudo, J. (2005) Bactericidal actions of a silver ion solution on *Escherichia coli*, studied by energy-filtering transmission electron microscopy and proteomic analysis. *Appl Environ Microbiol* **71**, 7589–7593.

Yan, L.Z., Chen, M.X., He, H. and Qu, J.U. (2005) Bactericidal effect of Al_2O_3-supported Ag catalyst. *Chin J Catal* **12**, 1122–1126.

Yang, C.M., Lin, H.A., Zibrowius, B., Spliethoff, B., Schuth, F., Liou, S.Z., Chu, M.W. and Chen, C.H. (2007) Selective surface functionalization and metal deposition in the micropores of mesoporous silica SBA-15. *Chem Mater* **19**, 3205–3211.

Zhang, L., Yu, J.C., Yip, H.Y., Li, Q., Kwong, K.W., Xu, A.W. and Wong, P.K. (2003) Ambient light reduction strategy to synthesize silver nanoparticles and silver-coated TiO_2 with enhanced photocatalytic and bactericidal activities. *Langmuir* **19**, 10372–10380.